

**RECEIVED**

**AUG 02 1999**

**OSTI**

**FINAL TECHNICAL REPORT**

## **Large Area Low Cost Processing for CIS Photovoltaics**

Submitted to: DOE/Oakland Office  
1301 Clay Street  
Oakland, CA 94612-5208

Submitted by: International Solar Electric Technology (ISET)  
8635 Aviation Blvd.  
Inglewood, CA 90301

July 22, 1999

Contributors: B. Basol, G. Norsworthy, C. Leidholm, A. Halani, R. Roe, V. Kapur

SBIR Phase II Contract No: DE-FG03-96ER82191  
Project Period: 8/13/96-3/31/99

## **DISCLAIMER**

**This report was prepared as an account of work sponsored by an agency of the United States Government. Neither the United States Government nor any agency thereof, nor any of their employees, make any warranty, express or implied, or assumes any legal liability or responsibility for the accuracy, completeness, or usefulness of any information, apparatus, product, or process disclosed, or represents that its use would not infringe privately owned rights. Reference herein to any specific commercial product, process, or service by trade name, trademark, manufacturer, or otherwise does not necessarily constitute or imply its endorsement, recommendation, or favoring by the United States Government or any agency thereof. The views and opinions of authors expressed herein do not necessarily state or reflect those of the United States Government or any agency thereof.**

## **DISCLAIMER**

**Portions of this document may be illegible in electronic image products. Images are produced from the best available original document.**

## SUMMARY

CuInSe<sub>2</sub> (CIS) and related compounds are important photovoltaic materials that have been successfully used for the fabrication of high efficiency polycrystalline thin film solar cells. Despite the impressive results achieved in the laboratory, however, commercialization of CIS based solar cells has been slow. One of the reasons for this is the fact that CIS film growth techniques employed in the research labs are based on vacuum approaches that are difficult and/or expensive to scale up. The objective of this Phase II SBIR program was to develop and demonstrate a low cost, non-vacuum deposition technique for the growth of photovoltaic-grade CIS absorber layers.

The technical approach taken in this program was to develop a method that could strictly control the stoichiometric Cu/In ratio in the CIS absorbers since this stoichiometric ratio greatly affects the electrical and optical properties of this group of materials. One other consideration was to demonstrate a coating technique that can, in principle, deposit the CIS absorbers on large area substrates of 4-8 ft<sup>2</sup> size. These goals were successfully reached and a patent application was submitted internationally describing the novel approach developed.

The technique involves four steps; i) preparation of a Cu-In alloy powder, ii) preparation of an ink using the Cu-In powder as the pigment, iii) deposition of the ink on the selected substrate in the form of a thin precursor layer, and iv) selenization of the precursor to form the desired CIS compound.

The specific tasks that were accomplished in this program were:

- i) A novel, low cost particle deposition technique was developed. The ability of this technique to strictly control the Cu/In ratio was demonstrated. Ability of the approach to coat large area substrates was confirmed.
- ii) CIS films with excellent mechanical integrity were deposited on Mo/glass substrates without any peeling problems. These layers were studied by SEM and XRD. They were found to be single phase.
- iii) Solar cells were fabricated on the CIS layers using CdS/ZnO window layers and a total area efficiency of 10.56%, and active area efficiency of 10.9% were demonstrated. Future work should concentrate on the densification of the compound layers for better cell performance.

The results obtained in this project are important for low cost CIS based PV module production. It should be noted that, although the total worldwide PV market has now approached the \$1 billion mark, the most important barrier to its explosive expansion is the cost of PV products which, at the present time, are competitive for many remote power applications but high for other potentially very large markets. All the projections indicate that thin film PV technologies based on low-cost processes can make low-cost PV a reality for both terrestrial and space applications.

## 1.0 INTRODUCTION

One approach taken to lower the cost of photovoltaic (PV) modules is the development of polycrystalline thin-film solar cells using group I-III-VI<sub>2</sub> compound absorber materials such as CuInSe<sub>2</sub> (CIS) and CuInGaSe<sub>2</sub> (CIGS). The great potential of these semiconductors for photovoltaic applications has already been demonstrated by the fabrication of over 18% efficient thin-film devices. Large area module efficiencies in excess of 10% have also been demonstrated.

Despite the impressive results obtained for laboratory devices, CIGS thin film PV modules have not yet been fully commercialized. Part of the reason for this lies in the nature of this multinary compound which has a complex phase diagram and composition-dependent electrically active native defects. Therefore, deposition techniques employed to grow this compound semiconductor on large area substrates have stringent requirements for stoichiometric control. So far, the techniques used to deposit the high quality CIGS films with controlled stoichiometry are costly vacuum processing approaches that involve evaporation or sputtering. In fact, the method that yielded the highest efficiency device is a multi-source evaporation technique that can not be readily scaled up for large-area, low-cost manufacturing.

Standard co-evaporation techniques are difficult to scale up because they can not coat large area substrates uniformly. Furthermore, CIGS growth requires the use of expensive elements such as In and Ga, and therefore, material utilization becomes a critical issue. It is possible, to a certain extent, to improve the materials utilization and the uniformity of the evaporation flux by designing and using long and linear evaporation sources. However, high cost of machinery, high heat loading from the Cu source, the necessity of keeping large area substrates uniformly heated under vacuum conditions, and the necessity to control constant and uniform evaporation fluxes over each evaporation source are some of the challenges faced by such a processing approach.

Two or three-stage processes that separate the film deposition step from the reaction and compound formation step may be better suited for large scale production because these techniques can use large area magnetron sputtering methods for the deposition of the precursor layers on un-heated substrates. However, the challenges faced in this case include; i) high cost of the machinery required, ii) poor utilization of the sputtering target material (typically <50%), iii) close control of the sputtering rate which may change with time as the shape of the racetrack changes, and, iv) sputtering flux uniformity along the race-track, especially near the two ends of a rectangular cathode.

As the brief review above demonstrates, development of a low-cost deposition approach that can deliver high quality CIGS absorbers on large area substrates would be very important for accelerating the commercialization of CIGS based PV modules. The present R&D effort addressed this important issue and aimed at the development of a simple, large area, non-vacuum deposition approach with high material utilization. The technique involves preparation of fine powders of Cu-In alloys, formulating inks using these powders, depositing the inks on substrates in the form of precursor layers and converting the precursor layers into solar-cell-grade CIS absorbers.

Since early 1980's, when the potential of thin-film CIS as a photovoltaic material was recognized, there has been several attempts to grow solar-cell-quality CIS type absorbers using some of the well known low-cost, large-area thin film deposition methods such as screen printing and slurry spraying. Although such techniques have been successfully used for the deposition of high quality CdTe absorbers, their utilization for chalcopyrite film growth for photovoltaic applications did not bear fruit until recently. In this section of the final report we will review some of the prior work on chalcopyrite film growth by a group of non-vacuum methods which can be classified as "particle deposition techniques".

Arita et al. mixed pure Cu, In and Se powders and milled this starting powder mixture in liquid medium to form a source material in the form of a screen printable paste [1]. Analysis of this paste showed the existence of CIS phase which apparently formed during the ball milling process through the reaction of Cu, In and Se powders. The paste was coated onto substrates and annealed at high temperatures for film fusing. However, this process did not yield solar-cell-quality CIS absorber layers. Vervaet et al. [2,3] and Casteleyn et al. [4] experimented with various screen printable paste compositions that contained starting powders of CIS rather than a mixture of the elements. Although film sintering and grain growth were observed under certain conditions, the films obtained after the high temperature post-deposition annealing step could not be used for high efficiency solar cell fabrication. The same group also attempted to formulate a paste using the mixture of Cu and In powders. The goal was to lower the sintering temperature required for the formation of a fused CIS layer. After screen printing the Cu+In paste on a substrate, Se was deposited over it and the whole structure was heated to form CIS. Reportedly the screen printing quality of the Cu+In paste was not good due to the large particle size of the In powder and the selenization step did not yield a single-phase compound.

The prior work reviewed above typically employed starting powders with relatively large particle sizes. These powders were then subjected to mechanical milling with the goal of forming a good quality paste or ink, containing sub-micron size particles. Mechanical milling can be effective in reducing the particle sizes of brittle materials such as Cu-Se, In-Se and CIS. However, in approaches employing In powders, for example, the particle size can not be reduced by standard milling since the soft material would tend to coat the milling media as well as the other particles in the formulation. Therefore, milling in such cases may actually result in particle size growth rather than reduction.

In this program we demonstrated a new CIS deposition method employing ink formulations containing Cu-In alloy particles. It should be noted that Cu-In alloys are rather brittle and can be efficiently milled to form inks which in turn can be deposited on large area substrates using low cost techniques.

## **2.0 TECHNICAL APPROACH**

The philosophy behind the technical approach of this work can be seen in Fig. 1 which shows the general processing sequence for CIS absorber growth.

The first step of the process depicted in Fig. 1 is the preparation of a Cu-In alloy powder. The idea behind the approach is to set, and effectively control, the stoichiometry of the compound to be grown, before the growth process, in the source material. Once a source material of the Cu-In alloy powder with the desired Cu/In ratio is prepared, this source material is subjected to a pre-deposition treatment in the second step of the process. During the pre-deposition treatment step, the alloy powder is milled and mixed with other necessary ingredients to form an ink or a paste that can be later deposited onto a selected substrate in the form of a thin precursor layer. Deposition of the precursor layer constitutes the third step of the process. The unique feature of the precursor layer of this process is its perfect stoichiometric uniformity in micro-scale as well as macro-scale. It should be appreciated that even if the precursor deposition approach results in poor thickness uniformity over large area substrates, the stoichiometry of the material would still be uniform since the chemical composition of

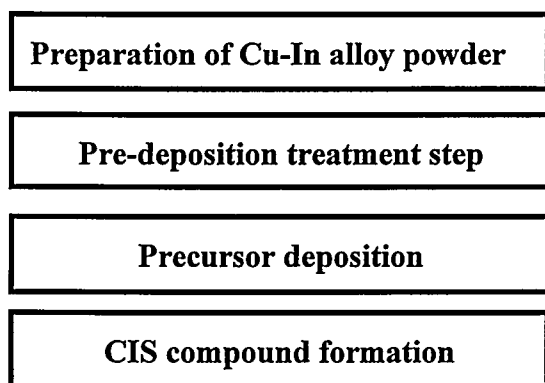


Fig. 1 The process sequence of the technical approach developed in this project for the growth of CIS absorber layers.

the source material is always uniform. The last step of ISET's new absorber growth process is the conversion of the precursor layer into the desired compound through a heat treatment step which involves selenization. Selenization of the precursor layers in this work was carried out in a reactor that employed 5% $H_2Se$ +95%  $N_2$  gas mixture. The selenization temperature was 440 °C and the typical selenization time was 30 minutes.

Solar cells with the glass/Mo/CIS/CdS/ZnO structure were fabricated on the CIS absorbers by depositing CdS buffer layers and ZnO window films. Thin layers (1500 Å) of CdS were coated by the commonly used chemical bath deposition technique. ZnO was grown by MOCVD. The details of the CdS and ZnO deposition techniques can be found in reference [5].

As can be seen from the brief review of the technical approach, the deposition technique of this project addresses three major areas of concern for the commercialization of CIGS PV products. First, the technique fixes the stoichiometry of the material before the deposition step and then transfers this fixed stoichiometry directly onto a substrate and eventually into the compound layer so that the stoichiometric control is absolute. Second, the technique does not use any expensive specialized vacuum equipment for the growth of the absorber layers. Third, the

technique is very versatile and through the use of methods such as screen printing and spraying it can process very large substrates without concern for stoichiometric control. Material utilization in these methods can be close to 100% since unused material can easily be recycled.

### **3.0 PROJECT OBJECTIVES**

The overall objective of this SBIR project was the development and demonstration of a novel, non-vacuum, low-cost deposition technique for CIS-type absorber growth for thin-film solar cell applications. The technical approach proposed to accomplish this goal has been briefly reviewed in Section 2.0. The following sections of the report will summarize the work carried out, the results obtained and the estimate of the technical and economic feasibility of the developed technology.

### **4.0 RESULTS AND DISCUSSION**

#### **4.1 Cu-In ink preparation and precursor deposition**

The melt atomization method was used to obtain Cu-In alloy powders with Cu/In molar ratios varying from about 0.80 to 1.2. In this approach, 99.99% pure Cu and In elements were weighed and mixed to fix the Cu/In ratio to the desired value. The starting mixture was then placed into the canister of a small size atomization reactor and melted under a H<sub>2</sub> blanket at a temperature of about 900 °C. After stabilizing the melt, the liquid alloy was sprayed and atomized through a high temperature nozzle into the tank of the reactor which was filled with Ar gas. Quenched powder then fell into the distilled water on the bottom of the tank for further cooling. The resulting powder was collected, dried and sieved to separate particles smaller than approximately 25 μm in size.

About 10 grams of the sieved Cu-In powder was mixed with 23 grams of water. A small amount (about 1.5% by weight) of a wetting agent and dispersant were added to this aqueous formulation. The mixture was milled in a ball mill for 42 hours. The resulting metallic ink was water-thin.

Glass/Mo substrates were prepared by depositing 0.5-3.0 μm thick Mo layers on 3 mm thick soda-lime glass sheets in an in-line D.C. magnetron sputtering system. Precursor films containing the milled Cu-In alloy pigment were coated over the glass or glass/Mo substrates by either doctor blading or spraying the formulated ink. After coating, the wet films were dried in a warm oven.

Table 1 shows the yield (in % weight) of the melt atomization approach for the fabrication of Cu-In alloy powders of various compositions. The histogram analysis for the -625 mesh powder sample is shown in Table 2. According to the data of Table 1, about 90% of the melt introduced into the canister of the reactor was transferred into -625 mesh powder which was used in the second step of the process. About 10% of



the melt was in the form of larger size particles. It should be noted that the material utilization at this stage of the process is 100% since the larger size particles can be readily fed into the melt canister for the next atomization run. Data of Table 2 shows that about 10% of the -625 powder is  $<4 \mu\text{m}$  in size, 50% is  $<10 \mu\text{m}$  and

Cu/In ratio	-625 mesh yield (%)	-400/+625 yield (%)	-100/+400 yield (%)	+100 yield (%)
0.87	89.6	5.6	4.3	0.5
0.98	89.3	5.4	4.7	0.6
1.05	89	5.5	5.1	0.5

Table 1 Yields in terms of particle size of the alloy powders with different compositions.

Cu/In ratio	90% $< (\mu\text{m})$	50% $< (\mu\text{m})$	10% $< (\mu\text{m})$	Mean $(\mu\text{m})$
0.87	24.4	11.5	4.5	13
0.98	24.1	11.2	4.4	12.8
1.05	25.5	10.7	4	12.8

Table 2 Histogram analysis of the -625 mesh alloy powders of various compositions obtained by the melt atomization technique.

90% is  $<25 \mu\text{m}$ .

A scanning electron micrograph of a typical Cu-In alloy powder sample after sieving is shown in Fig. 2. As can be seen from this figure, the particles forming the alloy powder are mostly spherical in shape and their sizes vary from about  $2 \mu\text{m}$  to  $25 \mu\text{m}$ .

The phase content of the starting alloy powder was studied by x-ray diffraction. The XRD pattern obtained from a sample of the powder of Fig. 2 is shown in Fig. 3. The experimentally found d-spacings and the peak intensities are given in Table 3, along with the phases that could possibly be assigned to this data. Clearly there is a pure In phase (JCPDS 5-642) in our starting powder. As can be seen from Table 3, the rest of the major peaks can be indexed to the Cu-rich phase of  $\text{Cu}_9\text{In}_4$  (JCPDS 42-1476). There is, however, the possibility of  $\text{Cu}_2\text{In}$  phase (JCPDS 42-1475) also, since peaks belonging to this phase at d values of 3.035, 2.142, 1.66 and  $1.516 \text{ \AA}$  overlap with the peaks of  $\text{Cu}_9\text{In}_4$ , and a small peak at the angle of  $52.17^\circ$  ( $d=1.752$ ) can be uniquely assigned to the  $\text{Cu}_2\text{In}$  phase. The peaks at d-spacings of 2.597, 2.331, 2.097, 2.086 and  $1.541 \text{ \AA}$  match well with the In-rich phase of  $\text{CuIn}_2$  [6,7]. The peak at around

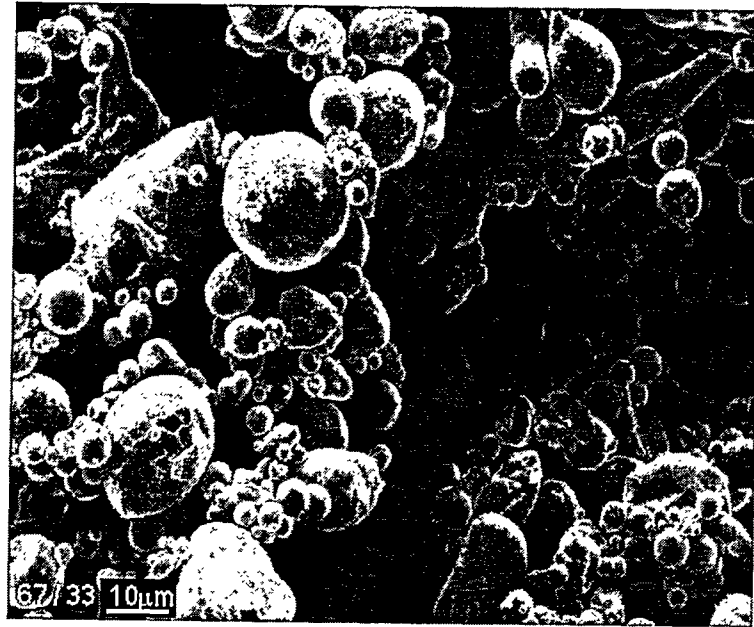


Fig. 2 SEM of a Cu-In alloy powder obtained by the melt atomization technique.

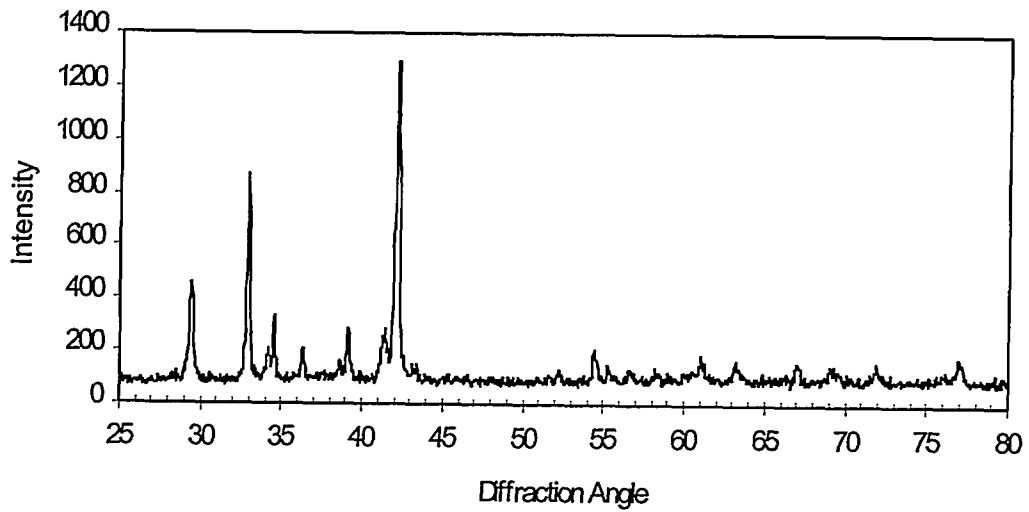


Fig. 3 XRD data taken from a powder prepared by the atomization of a Cu-In melt.

d (Å)	2θ (deg)	Intensity	In	Cu <sub>9</sub> In <sub>4</sub>	CuIn <sub>2</sub>
3.036	29.40	27		3.036 (75)	
2.72	32.90	76	2.715 (100)		
2.624	34.14	8		2.624 (75) [Lost after H.T.]	
2.597	34.50	25			2.601 (100) [Lost after H.T.]
2.473	36.29	12	2.471 (21)		
2.331	38.60	6			2.333 (24) [Lost after H.T.]
2.302	39.10	21	2.298 (36)		
2.182	41.35	9			
2.145	42.10	100		2.144 (100)	
2.097	43.09	7			2.10 (43) [Lost after H.T.]
2.086	43.35	7			2.09 (29) [Lost after H.T.]
1.752	52.17	4		1.750 (5) [Lost after H.T.]	
1.685	54.40	14	1.683 (24)		
1.661	55.25	6		1.660 (10) [Lost after H.T.]	
1.626	56.55	6	1.625 (12)		
1.583	58.22	5		1.584 (5) [Lost after H.T.]	
1.541	59.98	5			1.543 (31) [Lost after H.T.]
1.518	61.01	7		1.516 (50)	
1.471	63.13	7	1.47 (16)		
1.396	66.97	5	1.395 (23)		
1.359	69.04	7	1.358 (11)	1.356 (5)	
1.312	71.90	6		1.313 (15)	
1.238	76.98	7	1.237 (3)	1.238 (80) [Lost after H.T.]	

Table 3 A listing of the d-spacings and the peak intensities obtained from Fig.3. Phases that could be indexed to the data are shown with JCPDS d-values and intensities (in parentheses). Peaks that disappear upon heat treatment at 150 °C are also indicated.

41.35° could not be clearly identified. It may belong to the Cu-rich phase of  $\text{Cu}_{16}\text{In}_9$  (JCPDS 26-523).

As described before, our starting alloy powders were prepared by the melt atomization technique. In this method, the liquid droplets of Cu+In cool down rapidly in an inert gas, eventually falling down into a reservoir filled with distilled water at the bottom of the atomization unit. Therefore, existence of the highly Cu-rich phases in this quenched powder is not surprising. During the cool down period, after the rapid solidification of the high melting point Cu-rich phases, the remaining In-rich liquid apparently separated into the  $\text{CuIn}_2$  and In phases. To check the validity of the assignment of certain minor peaks to the  $\text{CuIn}_2$  phase, and to determine the origin of the peak at 41.35°, we annealed the powder sample of Fig. 3 in  $\text{H}_2$  atmosphere at 160 °C for about 30 minutes and obtained new XRD data from this annealed powder. The observations made on the XRD data of the annealed sample are presented in brackets in Table 3. It is seen that all the peaks assigned to the  $\text{CuIn}_2$  phase in the original powder disappeared as a result of the heat treatment step except for the peak at 34.5° which only got smaller. Peaks originally uniquely associated with the  $\text{Cu}_9\text{In}_4$  phase also disappeared. The unidentified peak at around 41.35° split into two dominant peaks upon heat treatment. All of the new peaks in the data of the annealed sample indexed well to the  $\text{Cu}_{11}\text{In}_9$  compound (JCPDS 41-883).

$\text{CuIn}_2$  alloy phase is meta-stable and it decomposes above 150 °C. Therefore, we can state that the starting alloy powders used in this work contained In+ $\text{CuIn}_2$  phases in addition to the Cu-rich phases of  $\text{Cu}_9\text{In}_4$ ,  $\text{Cu}_2\text{In}$  and possibly  $\text{Cu}_{11}\text{In}_9$ . Upon heat treatment,  $\text{CuIn}_2$  phase decomposed and  $\text{Cu}_{11}\text{In}_9$  and In phases became dominant.

Fig.4 shows the XRD data of a precursor film deposited on a glass substrate

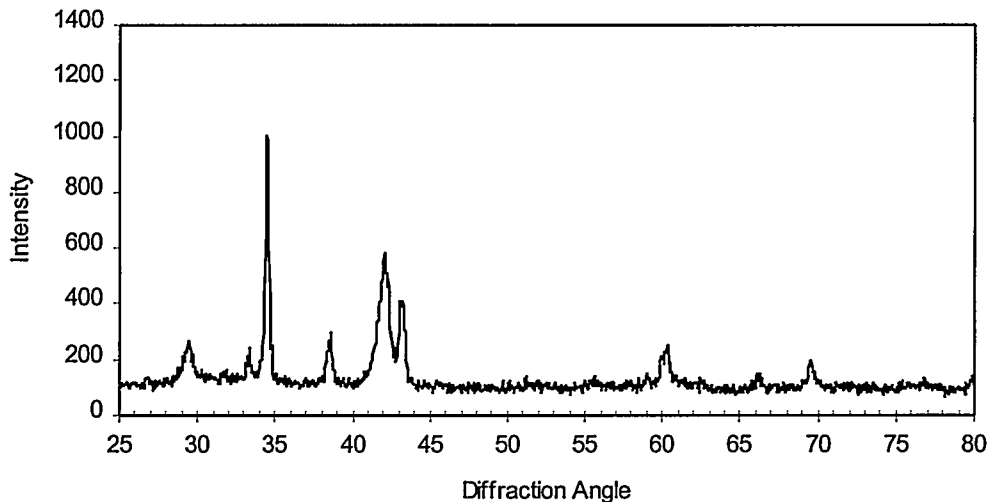


Fig. 4 XRD data obtained from the precursor layer deposited using the mechanically milled Cu-In ink.

d-spacing (Å)	2 $\theta$ (deg)	Intensity	CuIn <sub>2</sub>	Cu <sub>11</sub> In <sub>9</sub>
3.032	29.44	11		3.034 (80)
2.689	33.3	10	2.688 (12)	
2.6	34.46	100	2.601 (100)	
2.333	38.56	14	2.333 (24)	
2.150	41.99	18		2.145 (100)
2.137	42.26	14		2.136 (100)
2.101	43.02	21	2.101 (43) 2.09 (25)	
1.542	59.92	12	1.544 (31)	
1.534	60.29	14	1.535 (47)	
1.412	66.12	6	1.431 (31)	
1.351	69.5	13	1.353 (48)	

Table 4 A listing of the d-spacings and peak intensities obtained from Fig.4. The indexed phases are shown with JCPDS d-values and intensities (in parentheses).

using the milled Cu-In ink. Table 4 lists the experimental d-spacings and the phases that can be associated with this data. There are two observations one can make by comparing the XRD data of Figs. 3 and 4. The first observation is that the small CuIn<sub>2</sub> peaks found in the alloy powder of Fig. 3 grew appreciably in the sample of Fig. 4 in expense of the pure In peak which totally disappeared in Fig. 4. Also, the peaks associated with the Cu-rich phase became smaller and wider in Fig. 4, indicating poor crystalline quality and smaller grain size. Although the match of the dominant peaks in Fig. 4 to the calculated CuIn<sub>2</sub> powder diffraction data was excellent, the Cu-rich phase could only be approximately indexed to Cu<sub>11</sub>In<sub>9</sub>.

CuIn<sub>2</sub> phase has been observed in Cu/In film interfaces and the diffusion constants and activation energies have been calculated for the formation of this compound [6]. Apparently, in our ink making process, as the original alloy particles containing pure In, and Cu-rich and In rich phases got milled under the action of the heavy ceramic balls, the Cu-rich alloy phases reacted with the elemental In phase to form CuIn<sub>2</sub>. Since the temperature of the ink did not exceed 30 °C during the milling period, we attribute the observed phenomena to mechanical alloying. It is not uncommon to observe reactions promoted by the mechanical action of a ball mill. In fact, mechanical alloying in a ball mill was employed to form solid solutions of materials such as Fe-Cu, which are completely immiscible under normal equilibrium conditions [8]. It should be noted that when the film of Fig. 4 was later heated in an inert atmosphere to over 150 °C and then cooled down, the XRD pattern changed to one indicating the presence of only Cu<sub>11</sub>In<sub>9</sub> and In phases.

Presence of Cu-In alloys in the original metallic powder, micro-scale distribution of the pure In phase within each particle, and the reaction of the Cu-rich phases with In to form  $\text{CuIn}_2$  during milling are all highly desirable features of the reported technique. Vervaet et al. had previously reported that the quality of their pastes formulated from Cu and In powders was poor [2]. Our attempts to mill pure Cu and In powders to form metallic inks likewise did not yield good results because In is a soft metal. For such ink formulations, rather than particle size reduction, the milling process resulted in the formation of In flakes and eventual coating of the ceramic ball surfaces with In. In our present approach, the soft In phase is microscopically distributed in the particles containing the Cu-rich Cu-In alloys and it can be reacted with these Cu-rich alloys to form  $\text{CuIn}_2$ . The Cu-In alloys are more brittle than In. Therefore, particle size reduction could be achieved by milling the ink formulations using the alloy powders. Figure 5 shows the particle size distribution of a starting powder after sieving and in the milled ink, respectively. The frequency in Fig. 5 was calculated according to the number distribution mode. The mean particle size of this specific powder sample was found to be  $3.74 \mu\text{m}$  and the mean particle size in the milled ink was  $0.53 \mu\text{m}$ , clearly demonstrating particle size reduction.

Figure 6 is the cross sectional SEM of a Cu-In precursor film spray deposited on a glass/Mo substrate. The average thickness of this precursor layer is about  $4 \mu\text{m}$ . The alloy particles forming the film appear to be randomly shaped. Most of the particles are sub-micron size. However, there are also thin platelets which are as long as  $2 \mu\text{m}$ . These platelets form as the original rounded particles of Fig. 2 break under the action of the heavy ceramic balls during the milling step. Since the particles forming the precursor layer of Fig. 6 are randomly shaped, their packing density was low and this porosity carried on into the CIS film when the precursor was selenized in an  $\text{H}_2\text{Se}$  atmosphere as we will see later.

Large area deposition capability of the technique developed in this program was demonstrated by setting up a simple spray deposition system at ISET laboratory. The deposition equipment consisted of a fixed spray gun, a micro-pumping system that supplied controlled amounts of the formulated ink to the spray head and a substrate stage that moved under the spray gun at fully adjustable travel speeds. Substrates up to 1ftx2ft size could be coated in the small hood where this simple setup was placed. The system could, in principal, be used for coating much larger substrates as long as one dimension of the substrate was limited to 12 inches. Wider substrates could be coated by increasing the number of spray heads and micro-pumping systems.

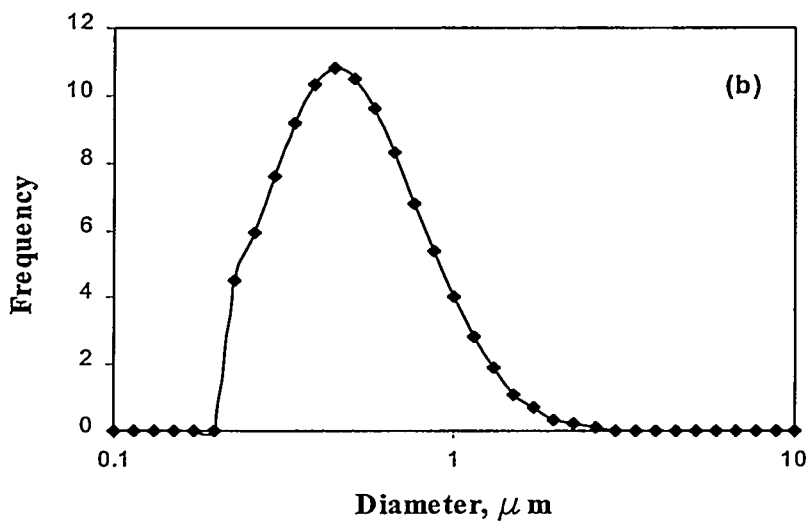
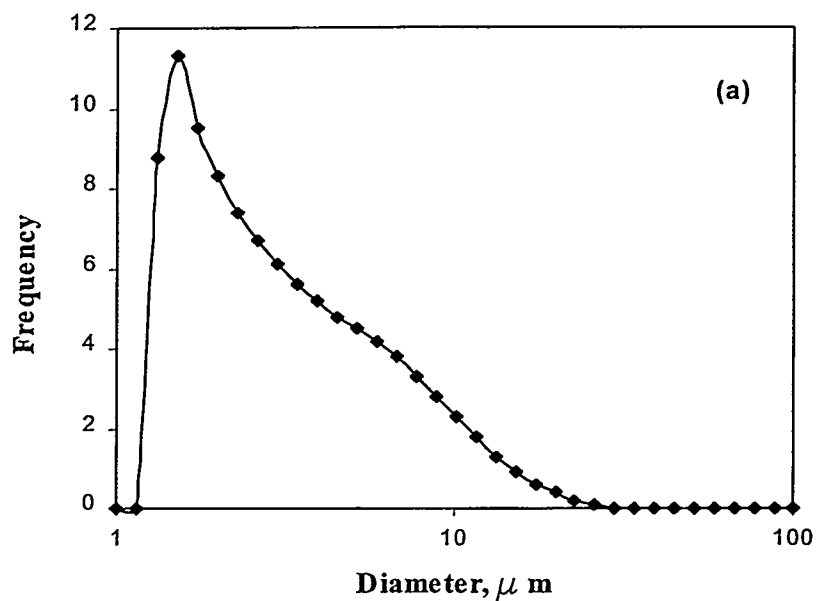


Fig. 5 Particle size distribution of a) starting sieved powder, b) powder in the milled ink.

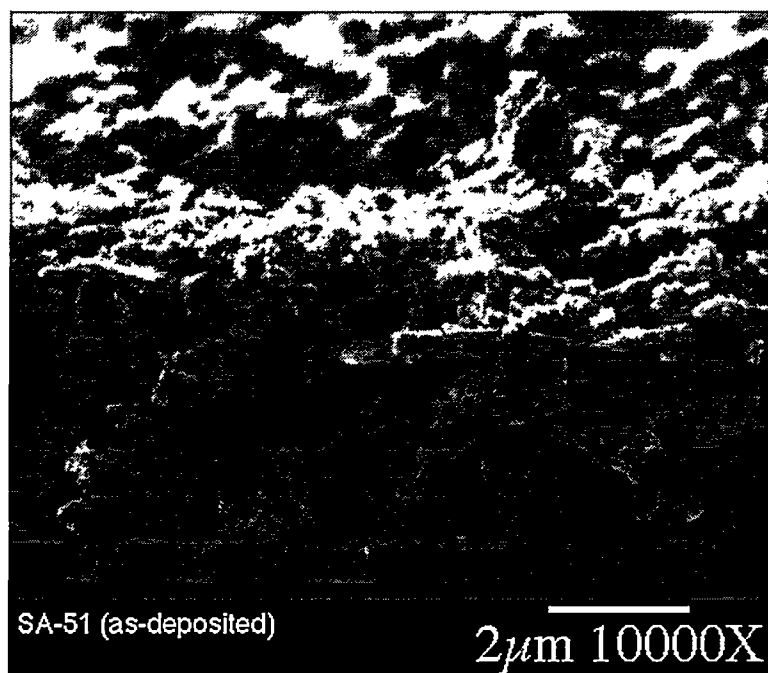


Fig. 6 Cross sectional SEM of a precursor film deposited by spraying a ball-milled Cu-In alloy ink.

#### 4.2 CIS absorber formation

The Cu-In alloy precursor layers coated on glass/Mo substrates were selenized in a 5% H<sub>2</sub>Se + 95% N<sub>2</sub> atmosphere at a temperature range of 400–450 °C for about 30 minutes. The resulting films were analyzed by SEM and XRD. The XRD pattern of Fig. 7 was taken from a selenized layer. All of the peaks in this pattern are associated with the chalcopyrite CIS phase and the Mo substrate. No other secondary phases were detected.

A Ga-containing ink was also formulated during this research program. However, the quality of this ink was not good for spraying because milling of the Cu-In-Ga pigments was not efficient. Precursor films were coated by the doctor blading technique on glass/Mo substrates and were selenized. The resulting compound layers contained both CIS and CIGS phases as indicated by XRD data. Efforts were then concentrated on CIS absorbers and their application to high efficiency solar cell fabrication.

The microstructure of the CIS films formed by the selenization of the precursor layers, such as the one depicted in Fig. 6, was found to depend on the composition of the starting powder. Figures 8a, 8b and 8c show the cross-sectional SEMs taken from CIS layers grown using inks with overall Cu/In ratios of 0.88, 0.98, and 1.05, respectively. In all cases, the crust of the CIS films is well fused and dense, but the bulk is porous. There is no clear grain structure that can be observed in the film with a Cu/In ratio of 0.88. The film with the Cu/In ratio of 0.98 has a visible network of consolidated regions, whereas filamentary grains of >1 μm can be observed around the voids in the Cu-rich absorber



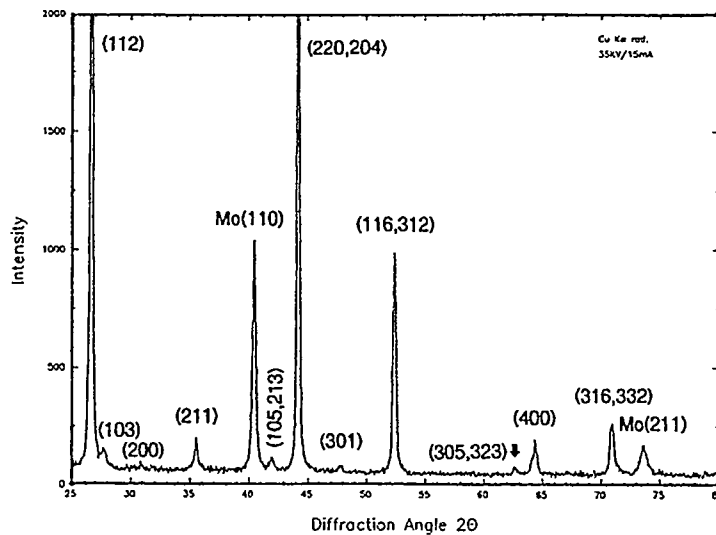


Fig. 7 XRD pattern of a CIS layer grown by the selenization of a sprayed Cu-In alloy precursor layer.

layer. Grain growth in Cu-rich CIS layers is due to the presence of excess CuSe phase with a low melting point. Presence of this phase promotes grain growth in films grown by evaporation techniques as well as the two-stage approaches.

The relatively porous films, such as the ones shown in Fig. 8, were successfully used to demonstrate high efficiency solar cells with conversion efficiencies in the range of 10-11%. The well fused, dense crust on the surfaces of these layers was adequate to make these active devices. However, long term stability of solar cells and modules would require reduction of internal surface area within the device structure. Our preliminary measurements on these porous devices indicated loss of current after exposure to long term illumination. Devices were under open circuit conditions and they were not laminated or otherwise protected from the environment during the experiment.

Densification studies were initiated to reduce porosity, improve the grain size and the morphology of the CIS layers grown by the ink spraying technique. Figure 9 shows an SEM of a selenized film which was compressed before the selenization step using a 3 cm diameter polished stainless steel ball race in an attempt to obtain a denser film. The pressure was estimated to be  $7 \times 10^4$  kN/m<sup>2</sup>, resulting in a reduction in thickness of the precursor film from 3.7  $\mu$ m to 2.5  $\mu$ m. The dense crystals forming a crust on the selenized film are approximately 50 % of the thickness of the film compared to approximately 15 % for the film which was not pressed.

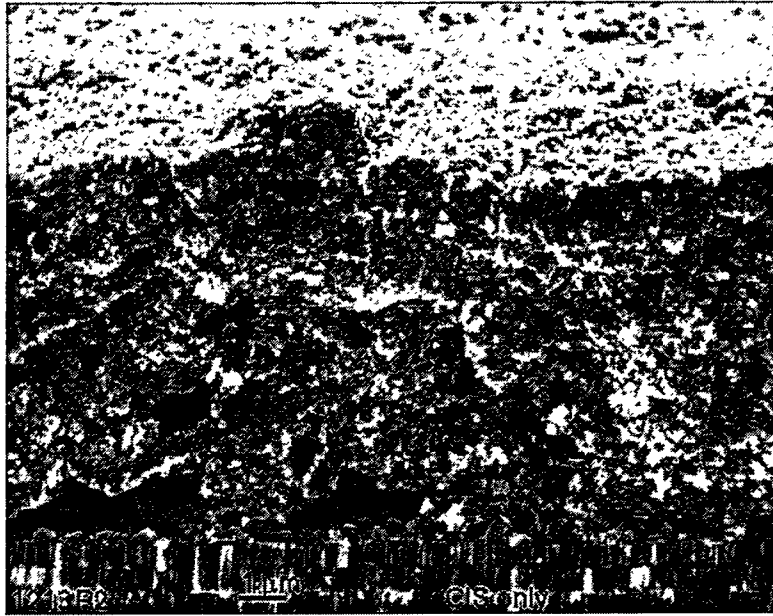


Fig. 8a Cross-sectional SEM (80 °tilt) of a CIS layer obtained by the selenization of a precursor with Cu/In ratio of 0.88.

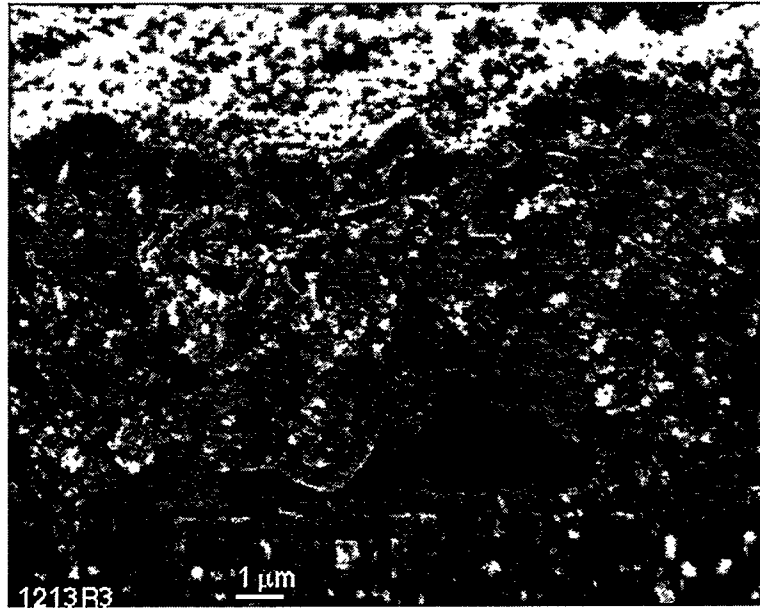


Fig. 8b Cross-sectional SEM (80 °tilt) of a CIS layer obtained by the selenization of a precursor with Cu/In ratio of 0.98.

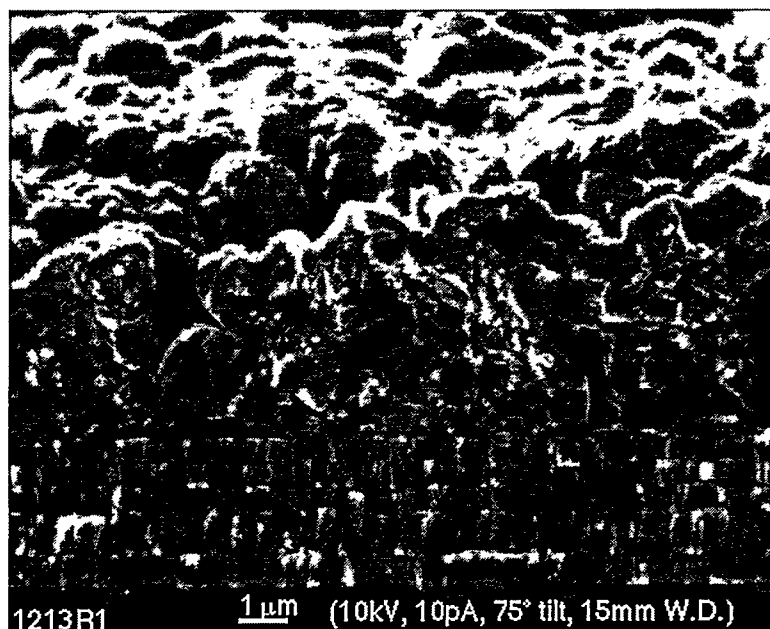


Fig. 8c Cross-sectional SEM (80 °tilt) of a CIS layer obtained by the selenization of a precursor with Cu/In ratio of 1.05.

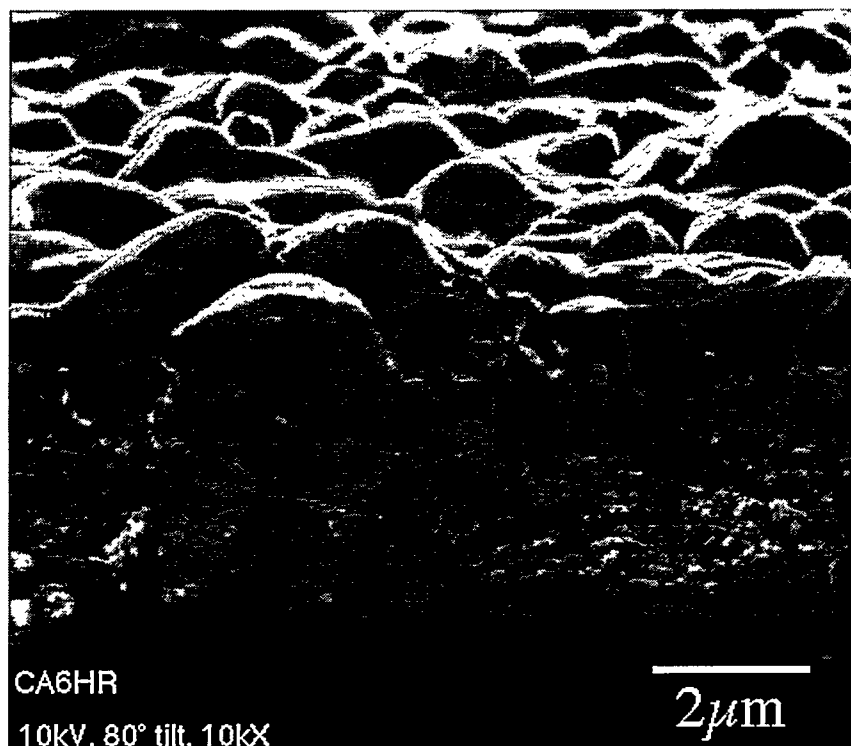


Fig. 9 Cross sectional SEM of a densified CIS layer. The precursor film was compressed after spray deposition and then selenized.

### 4.3 Solar cells

Solar cells were fabricated on the CIS films by depositing a 1000-1500 Å thick CdS layer by the chemical bath deposition (CBD) technique and a doped ZnO film by a MOCVD approach employing DEZ, water vapor and diborane. Devices were isolated through photolithography and etching, using masks with 0.09 cm<sup>2</sup> area. The shadow loss for probing was about 3%.

A complete set of solar cells were fabricated on films prepared using inks with Cu/In ratios of 0.87, 0.90, and 0.98. There was a definite trend of improved efficiency going from high Cu/In ratios to a Cu/In ratio of 0.87 and this was correlated with the compact surface layer of the highly In-rich films as we discussed previously. The solar cells fabricated on a layer with the Cu/In ratio of 0.88 yielded efficiencies in the 10-11 % range. Illuminated I-V characteristics of a cell measured at ISET under a solar simulator calibrated against AM1.5 spectra is given in Fig. 10. The efficiency of this 0.1 cm<sup>2</sup> area device is 10.56% with the open circuit voltage ( $V_{oc}$ ), short circuit current density ( $J_{sc}$ ) and fill factor (FF) values of 0.43 V, 37.5 mA/cm<sup>2</sup> and 65.5 %, respectively.

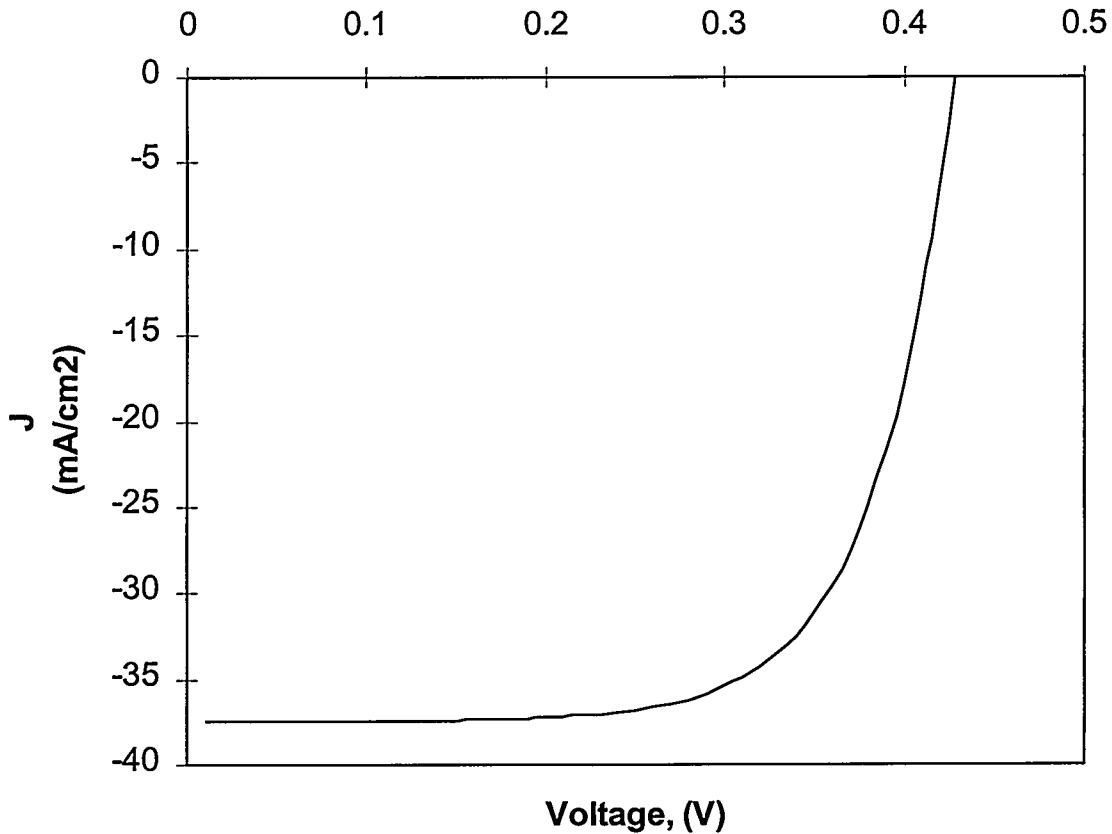


Fig. 10 Light I-V characteristics of a 0.1 cm<sup>2</sup> device that was fabricated on a CIS film with Cu/In ratio of 0.88.  $V_{oc}$ = 0.43V,  $J_{sc}$ = 37.5 mA/cm<sup>2</sup>, FF= 65.5%, EFF.= 10.56%.

Module integration studies were also initiated during this program. The integration procedure involved; i) Scribing of Mo to form Mo pads, ii) deposition of the precursor layer over the scribed Mo, iii) selenization, iv) CdS deposition, v) mechanical scribing to open vias through the CdS/CIS layers to expose Mo, vi) deposition of ZnO, and vii) mechanical scribing to isolate the adjacent cells.

While carrying out the module integration steps listed above, it was discovered that CIS film nucleation and growth within the scribed Mo lines, on the exposed glass surface was very different compared to growth on Mo surface. The resistivity of the material grown on the glass surface was low and it gave rise to low shunt resistance between the adjacent Mo pads. These issues can be addressed along with the issue of densification which will be discussed in the following section of the report.

## 5.0 CONCLUSIONS

A low cost technique based on "particle deposition" was developed and demonstrated for the growth of CIS-type, group I-III-VI<sub>2</sub> compound films, for photovoltaic applications. In this approach a starting metal-alloy powder with the desired (group I)/(group III) molar ratio was first prepared. Then an ink was formulated using this powder and well known ceramics techniques. The ink was coated on the glass/Mo substrates forming precursor layers composed of the nano-size particles contained in the ink formulation. Heat treatment steps with H<sub>2</sub>Se gas were used to convert the powdery precursor layers into solar-cell-grade chalcopyrite absorbers. Solar cells with conversion efficiencies in the range of 10-11% were demonstrated on the absorber layers grown by this low cost particle deposition technique.

Non-vacuum techniques based on nano-particle deposition, such as the one described in this report, are desirable for CIS-type solar cell manufacturing because they offer the possibility of low cost processing. Large-area, high-speed, low-cost methods, such as spraying, doctor blading and screen printing, can be used for the deposition of inks or pastes formulated with fixed composition.

International patent applications were prepared and submitted for the technology developed under this program. Notice of allowance has been recently received from the U.S. Patent Office. ISET believes that the developed technology will offer both economic and technical feasibility provided that further work is carried out on film densification. Porosity in CIS-type absorbers is expected to give rise to long term instabilities in the module structures. Therefore, the density of the films should be increased and procedures used for densification should be compatible with large area processing. ISET has plans for such a work which will also eliminate the shunting problem seen in module structures. Low cost photovoltaic modules fabricated using this low-cost particle deposition technique have a wide range of terrestrial applications ranging from small battery chargers to grid-connected power generation applications.

## 6.0 REFERENCES

1. T. Arita, N. Suyama, Y. Kita, S. Kitamura, T. Hibino, H. Takada, K. Omura, N. Ueno, and M. Murozono, Proc. 20th IEEE Photovoltaic Specialists Conf., IEEE, NY, 1988, p. 1650.
2. A. Vervaet, M. Burgelman, I. Clemminck and J. Capon, Proc. 9th EC Photovoltaic Solar Energy Conference, 1989, p.480.
3. A. Vervaet, M. Burgelman, I. Clemminck and M. Casteleyn, Proc. 10th EC Photovoltaic Solar Energy Conference, 1991, p.900.
4. M. Casteleyn, M. Burgelman, B. Depuydt, and I. Clemminck, Proc. 12th EC Photovoltaic Solar Energy Conference, 1994, p. 604.
5. B.M. Başol, V.K. Kapur, C.R. Leidholm, A. Halani, and A. Minnick, American Institute of Physics Conf. Proc. 353 (1996), p. 26.
6. W. Keppner, R. Wesche, T. Klas, J. Voigt and G. Schatz, Thin Solid Films, 143 (1985) 201.
7. C. Dzionk, H. Metzner, H.J. Lewerenz and H.E. Mahnke, J. Appl. Phys., 78 (1995) 2392.
8. F. Cardellini, V. Contini, G. D'Agostino and A. Filipponi, Materials Science Forum, 269-272 (1998) 473.